Virtual Tissue Electrical Properties: A New Concept for Fast, Robust Local SAR Estimation Based on B1 Measurement

Xiaotong Zhang[1], Pierre-Francois Van de Moortele[2], Jiaen Liu[1], Sebastian Schmitter[2], and Bin He[1,3]

[1]*Department of Biomedical Engineering, University of Minnesota, Minneapolis, MN, United States,* [2]*Center for Magnetic Resonance Research, University of Minnesota, Minneapolis, MN, United States,* [3]*Institute for Engineering in Medicine, University of Minnesota, Minneapolis, MN, United States*

PURPOSE: It has been shown that Electrical Properties (EPs) (conductivity σ, permittivity ε) of biological tissues can be derived from MR-based B1 measurement[1,2]. A strong appeal for these 'Electrical Property Tomography' (EPT) methods is to predict in real-time on a per-subject basis local SAR induced by RF pulsing. Two terms required to compute SAR are estimated by EPT: 1) Electric field (EF) and 2) EPs. EPs estimation however is typically highly sensitive to boundary conditions[3] in heterogeneous samples, and Laplacian based EPs reconstructions inherently amplify experimental noise. As a result, while acceptable in phantom or plain tissues, in-vivo EPT results are not satisfactory near tissue interfaces or in isolated sources of MR signal (e.g. scalp on skull). To reduce noise and artifacts, we eliminate the need for computing EPs by introducing the concept of 'virtual tissue EPs' (**V**EPs), tailored to provide max local SAR estimation based on measured B1 maps, with a safety margin. We evaluate the concept on electromagnetic models (EM) and *in-vivo* data of head imaging at 7T.

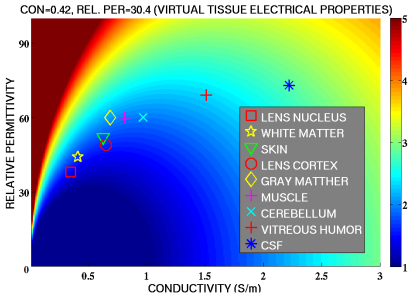

Fig.1. Overestimation Ω_V/Ω for head/neck tissues at 7T when VEPs are set to [σ_V=0.42Sm^{-1}, ε_V=30.4]. (Tissue EP values[4] considered with ±20% variation)

THEORY: SAR calculation can be written as $SAR=\sigma/2\rho(\mu^2\omega^2(\varepsilon-i\sigma/\omega)^2)\|\nabla\times\mathbf{B}\|^2=\Omega\|\nabla\times\mathbf{B}\|^2$ (Eq.1), where tissue-related variables are σ, ε and ρ (mass density) while μ (permeability) is assumed equal to free space. Angular frequency (ω) and RF coil induced magnetic field vector (**B**) are determined by coil sensitivity profile and RF pulse. For simplicity, we omit the spatial variable r and consider ω constant. Central hypothesis: for a given imaged sample, there exist some pairs of **V**EPs=(σ_V,ε_V), together with virtual tissue proton density ρ_V, such that the following inequality is always true: max(10g**V**SAR)≥[max(10gSAR)×10g*SM*] (Eq.2), where max(10g**V**SAR) and max(10gSAR) are the max of 10g averaged SAR values in the entire sample based, for 10g**V**ASAR via **V**EPs and ρ_V, and for 10gSAR via actual EPs and ρ maps. The positive safety margin 10g*SM* insures 10gSAR overestimation that can be tailored. For a single voxel (SAR instead of 10gSAR), we define a similar ratio: $SM=\Omega_V/\Omega$ with $\Omega_V=\sigma_V/2\rho_V(\mu^2\omega^2(\varepsilon_V-i\sigma_V/\omega)^2)$. **METHODS.** A pair of **V**EPs satisfying $\Omega_V/\Omega>1$ at 7T (ω=298MHz) was found after mapping *SM* for all brain/neck tissues EPs[4] (except fat) in an exclusive search varying σ_V [0→3Sm^{-1}] and ε_V [0→100] (~50,0000 pairs) with ρ_V uniformly set to 1000kg/m^3. As shown in Fig.1, with **V**EPs set to [σ_V=0.42Sm^{-1}, ε_V=30.4], $\Omega_V/\Omega>1$ for all tissues (e.g. 1.66, 2.07 and 2.81 in WM, GM and CSF, respectively). The goal is then to compute 10g**V**SAR and max(10g**V**SAR) by deriving EF from B1 field[2,5], using **V**EPs instead of computing EPs, and compare the results with target 10gSAR and max(10gSAR). ELLA (head, neck and shoulder) and DUKE (head and neck) models from Virtual Family[6,7] were loaded in a 16-ch microstrip Tx/Rx head coil[8] tuned to 298MHz in SEMCAD (Speag, Switzerland). Using the resulting B1 maps, 3 B_1 shim solutions[9-11] were applied: CP and CP2+ mode with incremental phase of 22.5° and 45°, respectively, and local B1 shim in center brain. The corresponding *target* SAR was computed via Eq.1, using simulated **B** (B_1 and B_Z), actual EPs and ρ. For **V**SAR, simulated B_1 (without B_Z) was used as well as **V**EPs, and ρ_V was set to 1000kg/m^3. To mimic real MR conditions, B1 maps were masked out in bone tissues; to avoid null SAR in bones, ρ_V was empirically set to 500Kg/m^3 in bone tissues. In addition, *in-vivo* data has been acquired on a human subject in a 7T scanner (Siemens) equipped with an elliptical 16-channel head Tx/Rx coil, as described in refs[2,5], with a resolution of 1.5x1.5x5 mm^3.

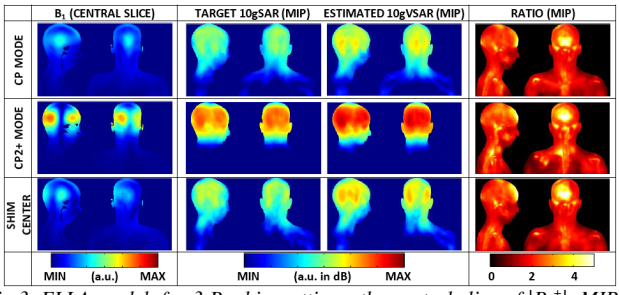

Fig.3. ELLA model, for 3 B_1 shim settings, the central slice of $|B_1^+|$, MIPs of target 10gSAR, estimated 10gVSAR, and 10gVSAR/10gSAR.

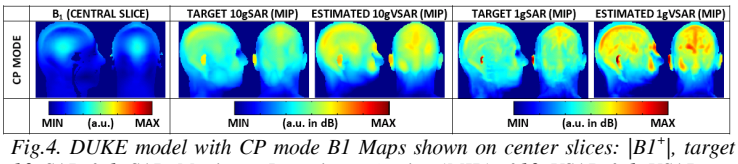

Fig.4. DUKE model with CP mode B1 Maps shown on center slices: $|B1^+|$, target 10gSAR & 1gSAR, Maximum Intensity projection (MIP) of 10gVSAR &.1gVSAR

RESULTS: A) Simulations. For three B_1 shim solutions, using the ELLA model, the overall overestimation of 10g**V**SAR vs. 10gSAR can be seen on max intensity projections (MIP) in Fig.3. Overestimation of 1g**V**ASR vs 1gSAR is also shown for DUKE model in CP mode in Fig.4. Table 1 summarizes, for each B_1 shim solution and both models, SAR overestimation obtained with 10g**V**SAR and 1g**V**SAR at the peak 1gSAR and 10gSAR hot spot locations, which quantifies the safety margin. Note that fat tissue (low EPs) was not considered when searching for optimum **V**EPs to avoid excessively high SAR overestimation. As a result, $\Omega_V/\Omega<1$ in fat may yield underestimated voxel-wise SAR for hot spots localized in fat tissue. However, 10g SAR averaging (official metric in IEC safety guidelines), effectively eliminated any occurrence of such underestimation due to averaging with neighboring tissues where $\Omega_V/\Omega>1$ (i.e. skin and muscle, see Fig.1); furthermore, even 1g**V**ASR always overestimated the more conservative 1gSAR. **b) *In-vivo* preliminary data** at 7T with a 16-ch Head coil: |B1+| map and 10g**V**SAR (including scalp and skull regions) derived from |B1+| are shown for two single coil elements (#3 & #11), to be compared with same maps from ELLA head model, on a slice exhibiting similar anatomical structures. Reasonable overall similarity is observed. Less reliable B1 measurement within scalp locally deteriorated 10g**V**SAR estimation, which is explained by the sensitivity of our current mapping sequence to scalp water/fat chemical shift, requiring further improvement.

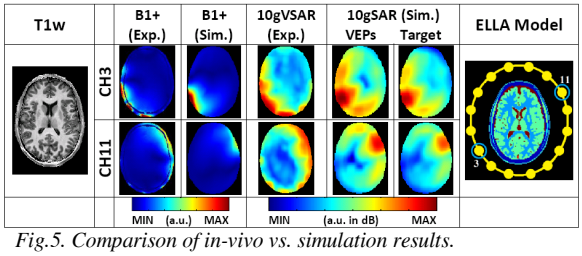

Fig.5. Comparison of in-vivo vs. simulation results.

Discussion: It had been proposed to use tissue EPs from the literature to get robust B1 map-based SAR prediction[2,5]. Here we entirely get rid of tissue specific EPs needs, using a unique pair of VEPs. We show that this allows to reasonably overestimate 10gSAR while avoiding deleterious consequences of errors in EPs reconstruction. The proposed technique still relies on B1 maps over the imaged volume, which can be addressed by implementing fast B1 mapping methods, while determining an optimal spatial resolution tradeoff. Other authors have proposed fast SAR computation based on a reduced number of EP compartments, using averaged actual EP values[12]; we believe that **V**EPs further simplify the problem and increased the degrees of freedom to find optimum tradeoffs between speed, robustness and patient safety. It will be interesting to see how this method applies to whole body strategies.

Table 1.Summary of max(local SAR) overestimation

EST. vs. TARGET PEAK LOCAL SAR		CP MODE	CP2+ MODE	SHIM CENTER
ELLA MODEL	*10gVSAR*	×1.36	×2.16	×2.08
	1gVSAR	×1.28	×1.79	×1.48
DUKE MODEL	*10gVSAR*	×1.46	×1.83	×1.50
	1gVSAR	×1.18	×1.33	×1.29

References: 1) Katscher, TMI 28:1365. 2) Zhang, TMI 32:1058. 3) Seo, TMI 31:430. 4) Gabriel, PMB 41:2271. 5) Zhang, MRM 69:1285. 6) Vaughan, John Wiley & Sons'12. 7) Christ, PMB 55:1767. 8) Adriany, MRM 59 :590. 9) Orzada, MRM 64:327. 10) Hetherington, MRM 63:9. 11) Schmitter, ISMRM'12 3472. 12) van den Bergen, PMB 54:1253.

Acknowledgment: NIH RO1EB006433, RO1EB007920, R21EB009133, R21EB014353-01A1 P41 RR008079, P41 EB015894, P30 NS057091, NSF CBET-0933067. We thank Dr. Xiaoping Wu for technical support.